



HAL
open science

Tridentate NNN Ligand Associating Amidoquinoline and Iminophosphorane: Synthesis and Coordination to Pd and Ni Centers

Louis Mazaud, Maxime Tricoire, Sophie Bourcier, Marie Cordier, Vincent Gandon, Audrey Auffrant

► **To cite this version:**

Louis Mazaud, Maxime Tricoire, Sophie Bourcier, Marie Cordier, Vincent Gandon, et al.. Tridentate NNN Ligand Associating Amidoquinoline and Iminophosphorane: Synthesis and Coordination to Pd and Ni Centers. *Organometallics*, 2020, 39 (5), pp.719-728. 10.1021/acs.organomet.9b00867 . hal-02919131

HAL Id: hal-02919131

<https://hal.science/hal-02919131>

Submitted on 16 Nov 2020

HAL is a multi-disciplinary open access archive for the deposit and dissemination of scientific research documents, whether they are published or not. The documents may come from teaching and research institutions in France or abroad, or from public or private research centers.

L'archive ouverte pluridisciplinaire **HAL**, est destinée au dépôt et à la diffusion de documents scientifiques de niveau recherche, publiés ou non, émanant des établissements d'enseignement et de recherche français ou étrangers, des laboratoires publics ou privés.

Tridentate NNN ligand associating amidoquinoline and iminophosphorane: synthesis and coordination to Pd and Ni centers.

Louis Mazaud,^a Maxime Tricoire,^a Sophie Bourcier,^a Marie Cordier,^a Vincent Gandon,^{a,b*} Audrey Auffrant^{a,*}

^a Laboratoire de Chimie Moléculaire, CNRS UMR 9168, École Polytechnique, Institut Polytechnique de Paris, 91128 Palaiseau, France

^b Institut de Chimie Moléculaire et des Matériaux d'Orsay (ICMMO), CNRS UMR 8182, Université Paris-Saclay, Bâtiment 420, 91405 Orsay cedex, France

ABSTRACT: The synthesis of a tridentate NNN ligand incorporating an amidoquinoline and an iminophosphorane (L^{RH} , $R = Ph, Cy$) was carried out. Coordination to Pd^{II} and Ni^{II} precursors gave as expected square planar complexes of general formula $[L^R MCl]$. The most surprising result came from the reaction of L^{PhH} with $[Ni(COD)_2]$ which gave a Ni^{II} -phenyl complex bearing a tridentate amidoquinoline-aminophosphine ligand. This rearrangement would result from a proton transfer assisted by the Ni^0 when stabilized by a phenyl substituent at the phosphorus, as suggested by DFT calculations and complementary experiments. This nickel-phenyl complex formed the corresponding benzoyl complex under a CO atmosphere.

INTRODUCTION

Pincer ligands are widely used in coordination chemistry because of their ability to coordinate a large variety of metals and the stabilization brought by the tridentate meridional anchoring points.¹ Moreover, the multiple synthetic possibilities to tune their steric and electronic properties, *via* the modification of the central coordinating atoms, the lateral ones and the linker between them allow adapting the ligand structure to the targeted applications. A large variety of NNN ligands offering only nitrogen coordinating atoms, was described. The most emblematic is maybe the terpyridine which has found numerous applications in catalysis, material science, and supramolecular chemistry.² The well-known bis(imino)pyridines, whose ability to store electrons was used to develop redox non-innocent base metal catalysts, belong to the same family.³ Possible architectures associating nitrogen heterocycles (pyridine, pyrrole, pyrazole, pyrazine), amine, imine, or amide are countless.⁴ However pincer structures incorporating electron-rich iminophosphorane ($N=P$) functions are by far less developed (see Figure 1). Bochmann and coworkers reported in 2000 the coordination of bis(iminophosphoranyl)pyridine derivatives (**A**) to iron, cobalt, and nickel centers and used those complexes for olefin polymerization.⁵ More recently we studied the coordination of the more flexible ligands **B** to lanthanides⁶ or electron-rich Cu^I centers.⁷ The ligand **C**, exhibiting a central anionic pyrrole in place of a pyridine, was employed by the group of Hayes to stabilize rare earth complexes⁸ or prepare Rh^I complexes able to promote CO activation in presence of borane.⁹ Ligands **D** with a nitrogen atom as linker between the $P=N$ functions were shown to stabilize rare earth¹⁰ or uranium¹¹ complexes while ligands **E** based on carbazole were coordinated to f-elements¹² as well as rhodium centers.¹³ The coordination of the neutral ligands **F** to

group 10 metal centers was studied by Stephan's group.¹⁴ A closely related ligand labelled **G** was synthesized by Alajarin *via* an original Michael addition of amine onto vinyliminophosphorane, and coordinated to cationic palladium centers.¹⁵

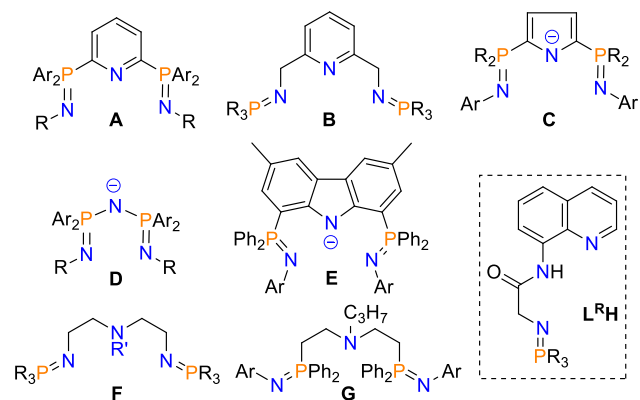
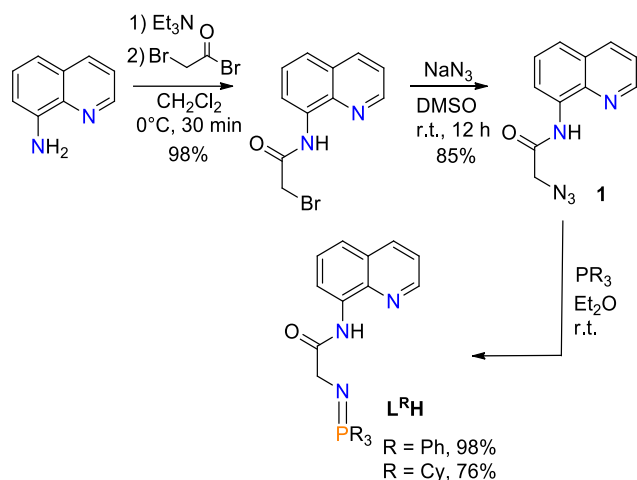


Figure 1: Tridentate NNN iminophosphorane based ligands

Given our continuous interest in developing new iminophosphorane ligand platforms,¹⁶ we describe herein the synthesis of tridentate NNN ligands associating an amidoquinoline and an iminophosphorane moiety. The first coordination experiments were conducted with Pd^{II} and Ni^{II} . The most surprising result came when reacting L^{PhH} with $[Ni(COD)_2]$ with the initial idea to isolate nickel-hydride complexes¹⁷ as already reported with other proton responsive functions.¹⁸ Instead we observed a rearrangement of the ligand, which mechanism was investigated by DFT-calculations, yielding a nickel-phenyl complex. Its carbonylation under CO giving the corresponding benzoyl nickel complex is also reported.

RESULTS AND DISCUSSION

Tridentate NNN ligand **L^{Ph}H** was easily synthesized thanks to a Staudinger reaction between triphenylphosphine and the azide **1** (Scheme 1). The latter was prepared in high yield by a procedure differing slightly from the one described by Chan and coworkers:¹⁹ 8-aminoquinoline was acylated with bromoacetyl bromide in presence of triethylamine to give, in 98% yield, 2-bromo-*N*-(quinolin-8-yl)acetamide, which was reacted with a slight excess of sodium azide in DMSO following Alvarez method²⁰ to deliver azide **1** in 85% yield. The Staudinger reaction between **1** and triphenylphosphine proceeded nicely in diethyl ether to give **L^{Ph}H** which was isolated as a white solid in 98% yield.



Scheme 1. Synthesis of **L^RH**

The workup was facilitated by its poor solubility in Et₂O allowing isolation by filtration. The formation of **L^{Cy}H** was achieved in the same manner but required less time (1 h vs 15 h) thanks to the better nucleophilicity of the tricyclohexylphosphine.

The IR spectrum of **L^{Ph}H** shows bands at 3230 and 1518 cm⁻¹ corresponding to the N-H bond, one at 1676 cm⁻¹ for the carbonyl bond and one at 1218 cm⁻¹ associated to the iminophosphorane bond.²¹ Moreover, **L^{Ph}H** is characterized in ³¹P{¹H} NMR spectroscopy by a singlet at 11.7 ppm in CD₂Cl₂ which is in the range of chemical shifts observed for free iminophosphorane of triphenylphosphine. In ¹H NMR spectroscopy, the methylenic protons resonate as a doublet at 3.89 ppm (³J_{P,H} = 15.0 Hz) and the amido proton as a broad singlet at low field (δ = 12.4 ppm). This is fairly deshielded compared to **1** (Δδ = 1.84 ppm) and may account for a hydrogen bonding between this proton and the nitrogen atom of the iminophosphorane.

This could be investigated thanks to X-ray diffraction. The structure of **L^{Ph}H** (see Figure 2) shows a planar molecule with a free iminophosphorane exhibiting bond and angle values typical of free iminophosphorane (P=N bond distance of 1.567(1) Å and an angle of 121.5° between the amido carbon, the phosphorus and the nitrogen). The short distance between the nitrogen of the iminophosphorane and the amido proton (2.1 Å) is in line with a weak interaction, as suggested by NMR data, but the three atoms are far from linearity (N-H-N 115.9°).

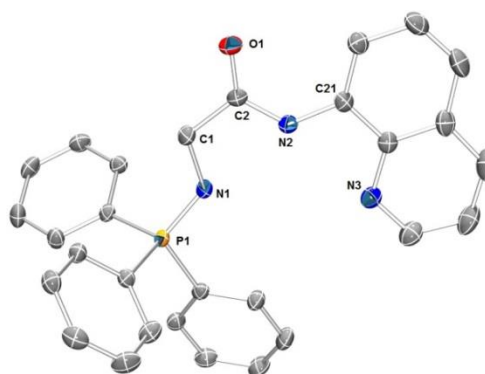
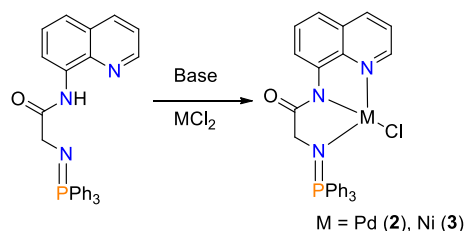


Figure 2. ORTEP plot of **L^{Ph}H**. Hydrogen atoms were omitted for clarity. Selected bond lengths (Å) and angles (°): P1–N1 1.567(1), P1–C3 1.805(2), O1–C2 1.229(2), N1–C1 1.453(2), N2–C2 1.354(2), N2–C21 1.396(2), C1–C2 1.515(2), N1–P1–C3 106.52(7), C1–N1–P1 121.5(1), C2–N2–C21 129.6(1), N1–C1–C2 112.1(1), O1–C2–N2 125.5(2), O1–C2–C1 121.1(1), N2–C2–C1 113.4(1).

The spectroscopic data for **L^{Cy}H** are very similar to that of **L^{Ph}H**. The only difference in the IR spectrum is the band corresponding to the iminophosphorane which appears at 1203 cm⁻¹ (vs 1218 cm⁻¹ for **L^{Ph}H**). In NMR, the differences are: the deshielded phosphorus (δ_P = 28.5 ppm) in line with previous reports,⁶ and the signals of the cyclohexyl protons between 1.2 and 2.3 ppm. The structure of **L^{Cy}H** (see Figure S1) was also analyzed by X-ray diffraction. This molecule is far less planar than its phenyl analogue (Figure S2) which is explained by the steric hindrance generated by the three cyclohexyl groups on the phosphorus. The P=N bond is also longer than in **L^{Ph}H** (1.580(1) vs 1.567(1) Å) as already observed for iminophosphoranes featuring alkyl groups on the phosphorus.⁶



Scheme 2. Coordination of **L^{Ph}** to Ni^{II} and Pd^{II}

The coordination study was focused on **L^{Ph}H**. Its deprotonation by one equivalent of KHMDS gave **L^{Ph-}**, with a phosphorus nucleus resonating as a broad singlet at 10.5 ppm in THF, which was then reacted with one equivalent of PdCl₂ at 40°C leading to **2** obtained as an orange solid in 50% yield after crystallization. The reaction could also be performed in presence of a weak base such as triethylamine. In NMR spectroscopy, the coordination results in a deshielding of the phosphorus nucleus, which resonates at 33.7 ppm, as well as that of the carbonyl (δ = 179.8 vs 174.3 ppm) and the methylenic carbon (60.9 vs 50.6 ppm). In this latter case, deshielding is accompanied by the extinction of the ²J_{P,C} coupling constant. In the ¹H NMR also, coordination induces a decrease of the ³J_{P,H} of the methylenic protons (4.5 vs 12.5 Hz) which are however slightly shielded after coordination (3.73 vs 3.89 ppm). The structure of **2** was further confirmed by X-ray diffraction analysis performed on single crystals obtained by slow diffusion of diethyl ether solution into

dichloromethane solution. The unit cell contains two slightly different molecules; one is presented Figure 3 and the second one in Figure S3. In this neutral complex, the palladium is coordinated to three nitrogen atoms of different chemical nature and a chloride. It therefore adopts, as expected for a d^8 metal center, a distorted square planar geometry, with the N3–Pd1–N1 and N2–Pd1–Cl1 measured respectively at 164.1 and 176.2°. The atoms linked to the metal and those of quinoline are coplanar, only C1 (0.47 Å), C2 (0.31 Å), and O1 (0.48 Å) are slightly distant from this plane. The central Pd1–N2 bond is slightly shorter (1.961(3) Å) than the lateral N1–Pd1 and N3–Pd1 ones of comparable length (2.029(3) Å), this is thus the strongest N–Pd bond of the molecule in agreement with the anionic character of N2. Upon coordination, there is not much change in the metrics of the amino-acetamide segment, while the iminophosphorane bond at 1.605 Å is, as expected, slightly elongated after coordination.

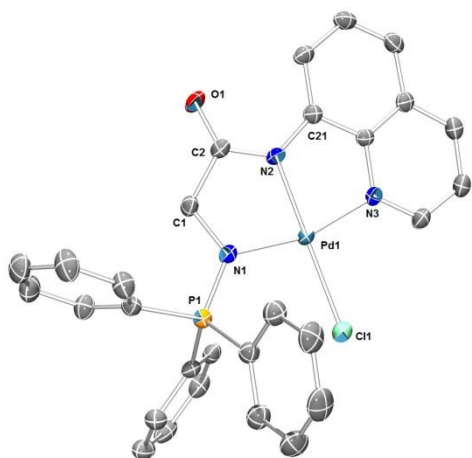
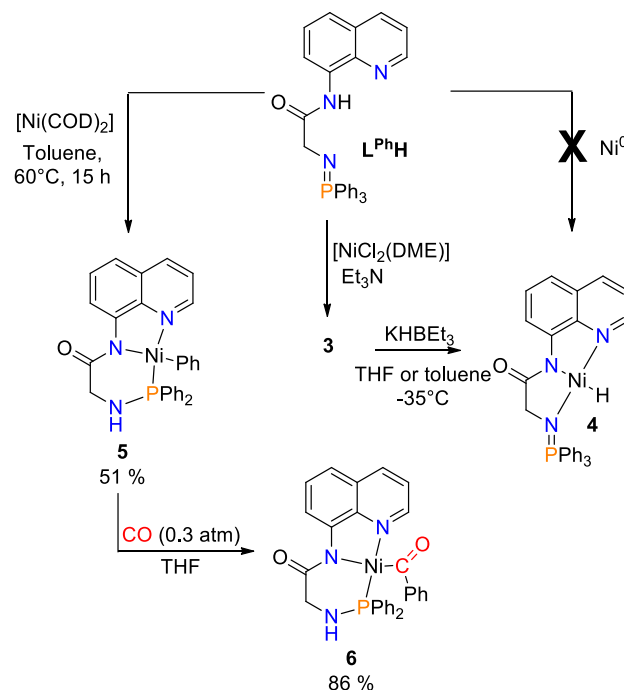


Figure 3. ORTEP plot of one molecule of **2**. solvent molecules and hydrogen atoms were omitted for clarity. Selected bond lengths (Å) and angles (°): Pd1–N2 1.961(3), Pd1–N3 2.029(3), Pd1–N1 2.029(3), Pd1–Cl1 2.330(1), P1–N1 1.605(3), O1–C2 1.229(4), N2–C2 1.349(4), N2–C21 1.397(4), N3–C1 1.473(4), C2–C1 1.518(4), N2–Pd1–N3 81.8(1), N2–Pd1–N1 82.4(1), N3–Pd1–N1 164.1(1), N2–Pd1–Cl1 176.21(8), N3–Pd1–Cl1 99.77(8), N1–Pd1–Cl1 96.09(8), C2–N2–C21 125.8(3), C2–N2–Pd1 118.4(2), C21–N2–Pd1 114.9(2), C1–N3–P1 119.6(2), C1–N3–Pd1 110.1(2), P1–N1–Pd1 127.9(2), N1–C1–C2 111.9(3).

Coordination to Ni^{II} was achieved by reacting L^{PhH} with $[NiCl_2(DME)]$ in THF in presence of a slight excess of triethylamine. After filtering off the ammonium salt, **3** was isolated in 90 % as a yellow solid, and characterized in $^{31}P\{^1H\}$ NMR as a singlet at 36.1 ppm, a chemical shift very similar to that observed for **2**. This points towards the formation of an analogous square planar diamagnetic Ni^{II} complex. The 1H and ^{13}C chemical shifts are also close to those of the palladium congener. Only the methylenic protons are pretty shielded with a resonance at 3.18 ppm vs 3.73 ppm in **2**. We tried to find an explanation to this observation but none were satisfying. The structure of **3** was further proved by X-ray diffraction analysis. It is very similar to that of the palladium analogue (see Figure S4) except that the coordination bonds are slightly shorter (- 6% on average) as expected since Ni^{2+} is smaller than Pd^{2+} .

Substitution of the chloride by a hydride was attempted with $KHBEt_3$ either in toluene or THF at $-35^\circ C$ (Scheme 3). Both reactions gave a sole product exhibiting a singlet at 30.5 ppm in

toluene. This product (**4**) could not be isolated since the filtration, evaporation of solvent and washing of the residue with pentane or diethyl ether led to a mixture of at least three products as judged by $^{31}P\{^1H\}$ NMR in which the initial product is still the major one. The hydride resonance could be observed as a doublet at -23.0 ppm ($^3J_{P,H} = 7.0$ Hz)



Scheme 3. Formation of complexes **5** and **6** and its carbonylation.

An alternative strategy to prepare a nickel hydride complex could be an oxidative addition of the N–H bond to electron-rich nickel center. Therefore L^{PhH} was reacted with $[Ni(COD)_2]$ (Scheme 3). Heating the reaction mixture in toluene at $60^\circ C$ overnight led to one phosphorous compound exhibiting a singlet at 72.4 ppm. This low field chemical shift compared to those of Ni^{II} or Pd^{II} complexes and the absence of hydride resonance clearly showed that the expected product was not formed. The 1H NMR characterization of the red solid obtained after work-up exhibited a doublet of triplets at 3.89 ppm ($J = 8.0$ Hz, $J = 5.0$ Hz) integrating for one proton, which couples with a doublet of doublets at 3.68 ppm ($J = 5.0$ Hz) integrating for two protons. These 1H chemical shifts are in line with those reported for aminophosphine.²² Moreover, ^{13}C NMR spectroscopy evidenced one additional quaternary aromatic carbon coupling with the phosphorus compared to **3**. In the IR spectrum, the N–H band appears at higher frequency (3209 cm^{-1}) compared to 3044 cm^{-1} in **3** and the carbonyl at 1577 vs 1617 cm^{-1} previously. The structure of this complex was finally elucidated thanks to X-ray diffraction analysis performed on single crystals obtained by cooling a concentrated toluene solution of the complex. The unit cell contains two independent molecules with similar parameters; one is presented in Figure 4 and the second one in Figure S5. The product of the reaction is a neutral Ni^{II} complex in a distorted square planar geometry resulting from the migration of one phenyl group from the phosphorus to the metal so that the iminophosphorane becomes an aminophosphine. Nickel in this complex labelled **5**, is therefore coordinated by the phosphorus, the nitrogen atoms from the amide and the quinoline and the carbon of the phenyl.

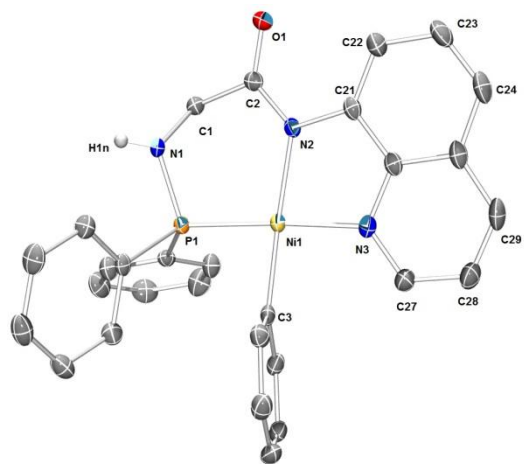
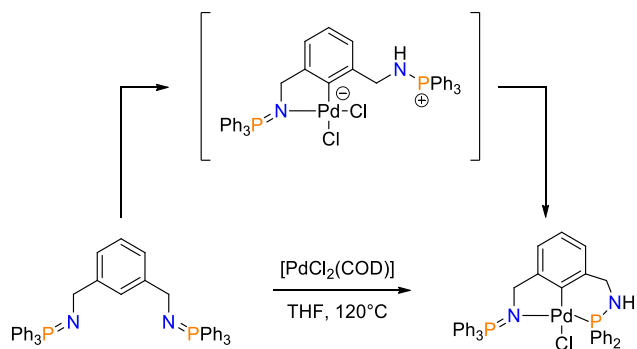


Figure 4. ORTEP plot of one molecule of **5**. All hydrogen atoms (except that of the aminophosphine) were omitted for clarity. Selected bond lengths (Å) and angles (°): Ni1–C3 1.895(2), Ni1–N3 1.946(2), Ni1–N2 1.959(2), Ni1–P1 2.121(6), P1–N1 1.663(2), O1–C2 1.240(2), N1–C1 1.462(2), N2–C2 1.360(2), N2–C21 1.419(2), C1–C2 1.525(3), C3–Ni1–N3 91.99(7), C3–Ni1–N2 171.57(8), N3–Ni1–N2 83.87(7), C3–Ni1–P1 84.72(6), N3–Ni1–P1 176.63(5), N2–Ni1–P1 99.31(5), N1–P1–Ni1 107.22(6), C1–N1–P1 115.0(1), C2–N2–C21 119.4(2), C2–N2–Ni1 129.0(1), C21–N2–Ni1 111.5(1), N1–C1–C2 113.2(2), N2–C2–C1 116.6(2).

The P–Ni bond measured at 2.121(3) Å is short compared to those described in the CCDC database for aminodiphenylphosphino nickel complexes (2.21 Å on average). Both N–Ni bonds are elongated comparing with those observed for **3** but the largest variation is seen for N2–Ni1 at 1.959 Å which is explained by the strong *trans* influence of the aryl ligand. The Ni1–C3 distance at 1.895 Å is comparable to that measured by van der Vlugt and coworkers on the only other example found in the CCDC database of a nickel–Ph complex with a pincer NNP ligand obtained *via* the photochemical CH activation of benzene by nitrido Ni complex.²³ The length of the P–N bond at 1.663(2) Å, is in the range of those measured for aminodiphenylphosphino nickel complexes (1.69 Å on average). This change in the nature of the phosphorous function induces also a slight elongation of the bonds within the aminoacetamide segment. This is due to the formation of a 6-membered metallacycle inducing a strong deformation from the ideal square planar geometry since N2–Ni1–P1 measures 99.3°. The methylenic carbon is also rejected away from the mean coordination, located at a distance of 0.62 Å from the P1–Ni1–N3–N2 plane (Figure S6). Because of steric hindrance, the phenyl ligand is almost perpendicular to this coordination plane (angle at 86.2°) and tilted from the plane defined by N2–Ni1–C3 (dihedral angle: 27.4°, Figure S6). The *ipso* carbon of this phenyl does not belong to the main coordination plane but is distant by 0.22 Å from it.

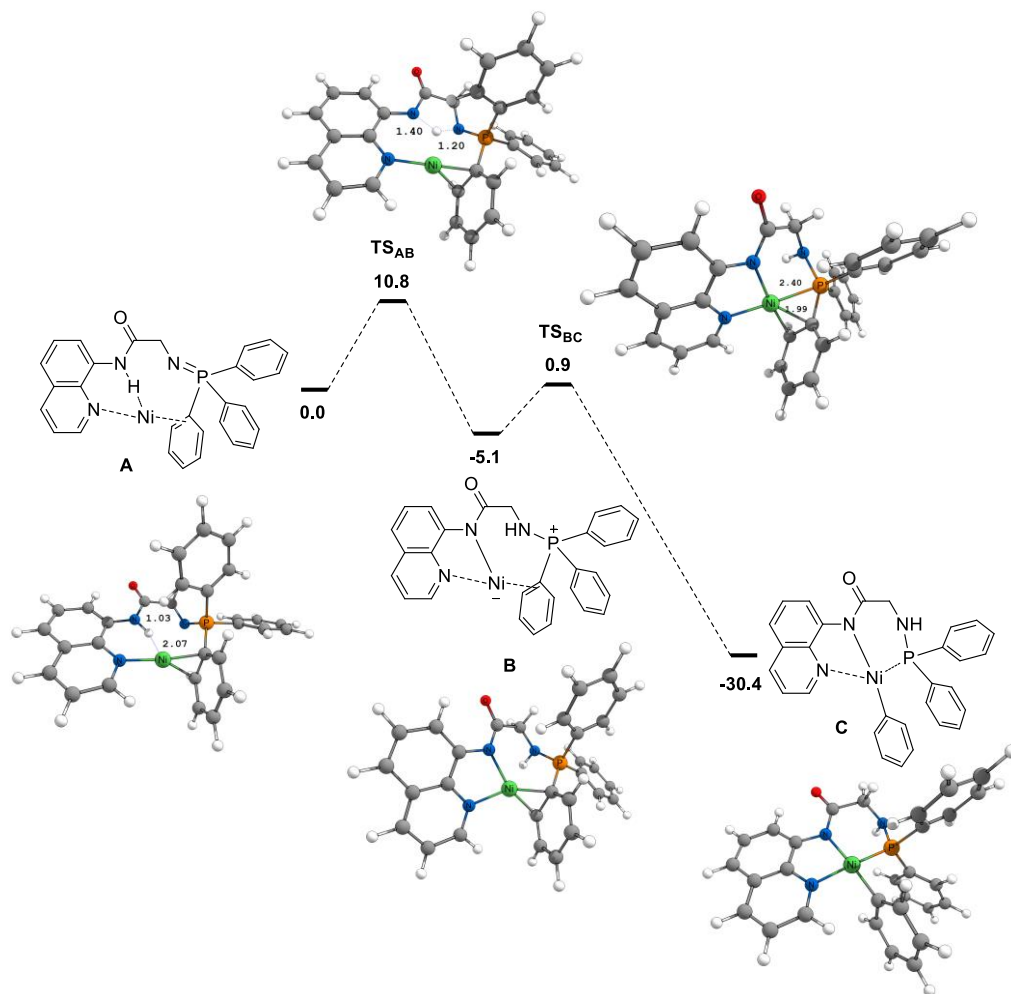
The only similar rearrangement we could find in the literature was reported by the group of Stephan in 2011 and occurred when heating a bis(iminophosphorane) NCN pincer ligand with [PdCl₂(COD)].²⁴ It was proposed to result from C–H oxidative addition of the arene *cis* to the iminophosphorane leading to a zwitterionic intermediate from which chlorobenzene is eliminated to afford the aminophosphine complex (Scheme 4).



Scheme 4: Previous example of iminophosphorane to aminophosphine rearrangement

This could not be confirmed by the characterization of the expected organic by-product. Given that precedent, we were curious to check whether the same rearrangement would take place with a Pd⁰ precursor. **L^{Ph}H** was reacted with [Pd₂(dba)₃] in toluene at 60°C leading to a mixture of products from which none could be isolated. The rearrangement we observed can hardly be compared to the previously known example (different metal, oxidation state, and ligand). Therefore, we conducted DFT calculations to shed light on the mechanism of this transformation.

Optimization of **L^{Ph}H** with Ni⁰ led to complex **A** (Scheme 5), in which the metal is ligated by the nitrogen atom of the quinoline moiety and π -linked to a phenyl group. The distance between the nickel center and the amide hydrogen is quite short (2.07 Å), but the N–H bond is only slightly elongated compared to a standard one (1.03 vs 0.99 Å). This suggests the presence of an electrostatic interaction between the negatively charged nickel (-0.130) atom and the positively charged amide hydrogen (0.353). The iminophosphorane nitrogen is too far from the metal to be engaged in bonding (3.11 Å). However, the closer amide nitrogen might become able to coordinate nickel if deprotonated. This deprotonation could actually be modeled through **TS_{AB}** in which the iminophosphorane nitrogen serves as a base. This transition state lays only 10.8 kcal mol⁻¹ above **A**. It connects **A** with the amide nickel(0) complex **B**. This step is exergonic by 5.1 kcal mol⁻¹. In the latter, the Ni–P distance is quite short, 2.90 Å. The Ni–P ligation is achieved after transferring a Ph group from the phosphonium center to the metal *via* **TS_{BC}**, which was located at 0.9 kcal mol⁻¹ on the free energy surface. The formation of the final and experimentally observed Ni^{II} complex **C** is markedly exergonic (30.4 kcal mol⁻¹ from **A**). The free energy of **TS_{AB}** is rather low for a reaction requiring heating at 333 K but the exchange of the cyclooctadiene ligands from [Ni(COD)₂] is endergonic by 14.3 kcal mol⁻¹ (Scheme S1). Thus, the barrier of the proton transfer when referenced to the reactants [Ni(COD)₂] and the iminophosphorane ligand is 25.1 kcal mol⁻¹. The entire process remains exergonic by 16.1 kcal mol⁻¹. Of note, the nickel atom cannot link with the amido and iminophosphorane nitrogen atoms when one COD is still present. Complex **D** was obtained as a η^2 -quinoline complex where the nickel is placed above the iminophosphorane ligand (see SI). From the calculations, the rearrangement is due to the electron-rich nickel atom assisting the proton transfer from the amido to the iminophosphorane nitrogen atom. We therefore controlled that this rearrangement cannot occur with Ni^{II} precursor. Indeed, heating **L^{Ph}H** and [NiBr₂(DME)] at 60°C in THF did not allow observing the formation of **5**.



Scheme 5. Free Energy Profile of the rearrangement (ΔG_{333} , kcal/mol)

Two ^{31}P resonances at 37.2 and 35.1 ppm are observed in the *in situ* $^{31}\text{P}\{^1\text{H}\}$ NMR spectrum, suggesting the formation of $[\text{L}^{\text{Ph}}\text{NiBr}]$ and the aminophosphonium $\text{L}^{\text{Ph}}\text{H}_2\text{Br}$ (L^{Ph} having served as a sacrificial base). Further heating to 110°C did not induce any change. As in the calculated intermediate **A**, the presence of the phenyl is important to stabilize the nickel center, we conducted a control experiment with $\text{L}^{\text{Cy}}\text{H}$. Its reaction with $[\text{Ni}(\text{COD})_2]$ leads to a mixture of products among which some are paramagnetic as attested by signals at low field in the *in situ* $^1\text{H}\{^{31}\text{P}\}$ NMR spectrum. Moreover, a singlet can be seen at -22.8 ppm and may account for the formation of a hydride complex. All our attempts to isolate those products remain vain. Only the structure of one product formulated as $[(\text{L}^{\text{Cy}})_2\text{Ni}]$ can be obtained (see Figure S7). Nevertheless, this confirms the important role of the phenyl substituents of the phosphorus in the formation of **5** as proposed by the calculations.

The reactivity of nickel-phenyl complexes in presence of carbon monoxide was studied in the context of nickel catalyzed ethylene/CO copolymerization and (de)carbonylation.²⁵ We were therefore curious to test if **5** could cleanly form the corresponding acyl complex. Indeed, the reaction, performed in a J. Young valve NMR tube, is rapid at room temperature under 0.3 bar of CO leading to a sole product characterized by a singlet at 70.0 ppm. However, the ^1H NMR shows only two multiplets integrating for one proton each at 4.14 and 3.97 while 3 protons (CH_2 and NH) should be observed in this region. Actually 2D

^1H - ^{13}C correlation experiments show that the methylenic carbon resonating at 52.2 ppm correlates with the signal at 3.97 and 3.55 ppm, which overlaps with the solvent peak. In ^{13}C NMR, a doublet at 256.6 ($^2J_{P,C} = 37.5$ Hz) confirmed the incorporation of carbon monoxide. This low-field chemical shift is in line with that reported for other Ni^{II} benzoyl complexes.²⁶ This is also clear from the IR spectrum evidencing a new intense band at 1600 cm^{-1} for COPh ligand while a less intense one at 1587 cm^{-1} corresponds to the amide CO bond. The NH of the aminophosphine gives bands at 3293 and 1563 cm^{-1} which are slightly shifted compared to **5**. The structure of **6** could be analyzed by X-ray diffraction. In this complex, the Ni^{II} adopts a distorted square planar geometry, the N2-Ni1-P1 angle measuring 97° . The benzoyl ligand is located *trans* to the amide nitrogen. The coordination bonds as well as the P-N one are very close to those measured for **5**. The Ni-C(O) bond length (1.860 \AA) is in the range of those measured in the six other examples of nickel benzoyl complexes found in the CCDC database (1.864 \AA on average).²⁷ The benzoyl points away from the phosphorus because of the steric hindrance due to the phenyl substituents, the angle between Ni1-C3-O2 and the benzoyl plane being at 20.6° . Because of the constraint due to the 6-membered metallacycle in **5**, the N and P atoms of the aminophosphine and the CH_2O are located on opposite sides of the N3-C3-Ni1-N2 plane (Figure S8), the distances to this mean plane are P1 (0.616 \AA), N1 (0.561 \AA), C1 (0.527 \AA), C2 (0.397 \AA) and O1 (0.702 \AA).

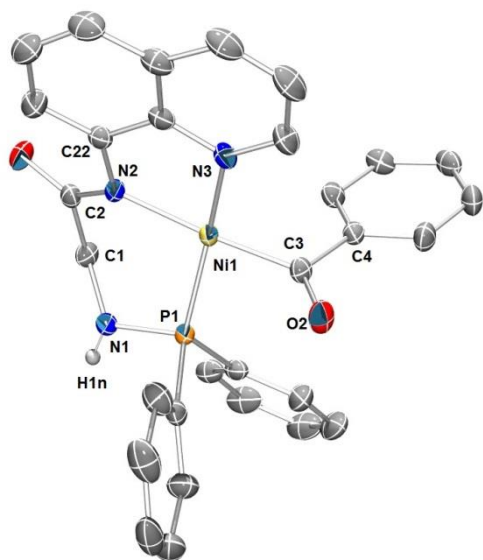


Figure 5. ORTEP plot of one molecule of **6**. All hydrogen atoms (except that of the aminophosphine) were omitted for clarity. Selected bond lengths (Å) and angles (°): Ni1–C3 1.860(2), Ni1–N3 1.9458(17), Ni1–N2 1.9572(16), Ni1–P1 2.1316(5), P1–N1 1.6620(17), O1–C2 1.233(2), O2–C3 1.224(2), N1–C1 1.460(3), N2–C2 1.359(2), N2–C22 1.406(2), C1–C2 1.526(3), C3–Ni1–N3 92.10(8), C3–Ni1–N2 175.90(8), N3–Ni1–N2 84.21(7), C3–Ni1–P1 87.47(6), N3–Ni1–P1 164.32(5), N2–Ni1–P1 96.57(5), N1–P1–Ni1 107.23(6), C1–N1–P1 119.05(14), C2–N2–C22 119.4(2), C2–N2–Ni1 129.0(1), C22–N2–Ni1 111.63(12), N1–C1–C2 114.10(16), O1–C2–N2 126.40(19) N2–C2–C1 116.32(16).

Contrary to CO, CO₂ could not be inserted when placing **5** under 0.3 bar of CO₂, but carboxylation generally occurs with alkyl complexes at higher pressure. We will have to pursue our investigations in that direction.

CONCLUSION

To conclude, we described the straightforward synthesis of a new tridentate pincer ligand associating three chemically different nitrogen atoms: one from a quinoline, one amide and one iminophosphorane. Two ligands differing by the nature of the phosphorus substituents (either phenyl (**L^{Ph}H**) or cyclohexyl (**L^{Cy}H**)) were prepared. Preliminary coordination tests were conducted with Group 10 metals. Reaction with [NiCl₂(DME)] and PdCl₂ precursors in presence of a base led to [**L^{Ph}MCl**] (**2**, M= Pd, **3** M= Ni) which were thoroughly characterized including X-ray crystallography. The formation of the hydride complex [**L^{Ph}NiH**] (**4**) was observed upon reaction of **3** with a hydride donor; nevertheless this complex could not be isolated. In order to form **4** by an alternative route, [Ni(COD)₂] was reacted with **L^{Ph}H**. The outcome of this reaction was surprising since the anticipated insertion of the metal into the N-H bond does not take place. Instead, an aminophosphine nickel(II) phenyl complex labelled **5** was formed. The mechanism of this transformation investigated by DFT calculations shows that the proton transfer from the amido to the iminophosphorane nitrogen atom is assisted by the electron-rich Ni⁰. Thus, the basicity of the P=N function cannot be neglected when coordinating iminophosphorane ligand featuring acidic protons. In that rearrangement the phosphorus substituents, belonging to the second coordination sphere, deeply influence the outcome of the reaction.

The phenyl substituents are necessary to stabilize the Ni⁰ intermediate. Their role is here different from tuning the electronic properties of the P or N atoms as commonly observed. These observations could open new possibilities regarding the coordination chemistry of ylide ligands with electron-rich metal precursors.

EXPERIMENTAL SECTION

General considerations. All reactions were conducted under an atmosphere of dry nitrogen, or argon, using standard Schlenk and glovebox techniques. Solvents and reagents were obtained from commercial sources. Solvents were distilled from a benzophenone/sodium solution or dried with a M-Braun MB-SPS 800 solvent purification system, transferred to the glovebox without exposure to air, and stored over molecular sieves. Deuterated solvents were used as received and stored over molecular sieves and sodium (where appropriate). All other reagents and chemicals were obtained commercially and used without further purification. Nuclear Magnetic Resonance (NMR) spectra were recorded on a Bruker Avance 300 spectrometer operating at 300 MHz for ¹H, 75.5 MHz for ¹³C and 121.5 MHz for ³¹P. Solvent peaks were used as internal references for ¹H and ¹³C chemical shifts (ppm). ³¹P{¹H} NMR spectra are relative to a 85% H₃PO₄ external reference. Unless otherwise mentioned, NMR spectra were recorded at 300 K. Coupling constant are expressed in hertz. The following abbreviations are used: br, broad; s, singlet; d, doublet; dd, doublet of doublets; t, triplet; m, multiplet; v, virtual. The spectra were analyzed with MestReNova software. The labelling used is indicated in Figure 6. Elemental analyses were performed by the Elemental analysis service of the London Metropolitan University (United Kingdom). Mass spectrometry experiments were recorded on tims-TOF mass spectrometer (Bruker, France). Samples are prepared in CH₃CN and introduced at 5 μL·min⁻¹ flow rate into the electrospray ion (ESI) source in positive mode. Accurate masses and elemental compositions were obtained using the DataAnalysis software. The elemental compositions were obtained with a tolerance below 5 ppm.

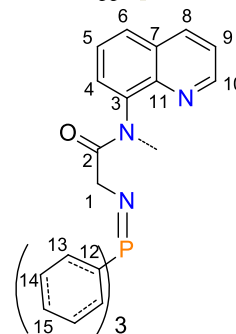


Figure 6. Labelling used for **L^R** moiety

2-bromo-N-(quinolin-8-yl)acetamide: 8-aminoquinoline (5 g, 34.7 mmol) was dissolved in dry CH₂Cl₂ (200 mL) and cooled to 0 °C before the addition of triethylamine (5.1 mL, 36.6 mmol) and that of 2-Bromoacetyl bromide (1.332 mL, 38.2 mmol) dropwise over 20 minutes. The resulting mixture was allowed to stir at 0 °C for further 10 minutes at which point full conversion was observed by TLC (eluent CH₂Cl₂). Water (100 mL) was added, the phases were separated, and the aqueous phase was extracted with CH₂Cl₂ (3 x 50 mL). The combined organic fractions were washed with brine, dried over MgSO₄, filtered through a pad of celite to remove solid impurities and concentrated under reduced pressure to yield 2-bromo-N-(quinolin-8-yl)acetamide as a brown solid (9.00 g, 98 %). ¹H NMR (CDCl₃): δ 10.74 (bs, 1H), 8.86 (dd, *J*_{HH} = 4.5 and 1.5 Hz, 1H), 8.74 (vdd, 1H), 8.19 (dd, *J*_{HH} = 8.5 and 1.5 Hz, 1H), 7.57-7.55 (m, 2H), 7.49 (dd, *J*_{HH} = 8.5 and 4.5 Hz, 1H), 4.15 (s, 2H).

2-Azido-N-(quinolin-8-yl)acetamide: 2-bromo-N-(quinolin-8-yl)acetamide (2.16 g, 8.16 mmol) was dissolved in DMSO (60 mL) and

sodium azide (0.78 g, 12.0 mmol) was added. The reaction mixture was stirred until full conversion observed after *ca.* 2 h by TLC (eluent: Pentane (8) : Et₂O (2)). Water (100 mL) and Et₂O (200 mL) were added, the phases were separated, and the organic phase was washed with water (2 x 150 mL) and brine (150 mL). The organic phase was then dried over MgSO₄ and concentrated under reduced pressure to yield 2-azido-N-(quinolin-8-yl)acetamide as an off-white to orange solid (1.55 g, 85 %). ¹H NMR (CDCl₃): δ 10.57 (bs, 1H, NH), 8.87 (dd, ³J_{HH} = 4.0 Hz and ⁴J_{HH} = 1.5 Hz, 1H, H₁₀), 8.76 (vdd, 1H, H₆), 8.18 (dd, ³J_{HH} = 8.5 Hz, ⁴J_{HH} = 1.5 Hz, 1H, H₈), 7.57–7.55 (m, 2H, H_{4,5}), 7.49 (dd, ³J_{HH} = 8.5 Hz, ³J_{PH} = 4.0 Hz, 1H, H₉), 4.27 (s, 2H, H₁). ¹³C NMR (CDCl₃): δ 165.1, 148.8, 138.7, 136.5, 133.6, 128.1, 127.3, 122.6, 121.9, 116.9, 53.7. HRMS (ESI⁺): 228.0887 ([MH]⁺; C₁₁H₁₀N₅O⁺; calcd 228.0880).

L^{Pb}H: 2-azido-N-(quinolin-8-yl)acetamide (1.55 g, 6.82 mmol) was dissolved in Et₂O (80 mL) and triphenylphosphine (1.79 g, 6.83 mmol) was added under vigorous stirring resulting in a small nitrogen evolution. The reaction mixture was stirred under nitrogen flux during 1 h and then closed. A white precipitate appeared after overnight stirring. The white solid was filtered, washed with Et₂O (2 x 40 mL) and petroleum ether (2 x 40 mL), and then dried *in vacuo* to yield **L^{Pb}H** (3.10 g, 98 %). ³¹P{¹H} NMR (CD₂Cl₂): δ 11.7 (s). ¹H NMR (CD₂Cl₂): δ 12.40 (bs, 1H, NH), 8.90 (dd, ³J_{HH} = 4.0 Hz, ⁴J_{HH} = 1.5 Hz, 1H, H₁₀), 8.81 (m, 1H, H₆), 8.20 (dd, ³J_{HH} = 8.5 and 1.5 Hz, 1H, H₈), 7.92 – 7.78 (m, 6H, H₁₃), 7.64 – 7.44 (m, 12H, H_{4,5,9,14,15}), 3.89 (d, ³J_{PH} = 12.5 Hz, 2H, H₁). ¹³C NMR (CD₂Cl₂): δ 174.3 (d, ³J_{PC} = 24.5 Hz, C₂), 148.9 (s, C₁₀), 139.7 (s, C₁₁), 136.7 (s, C₈), 135.8 (s, C₃), 133.1 (d, ²J_{PC} = 9.0 Hz, C₁₃), 132.2 (d, ⁴J_{PC} = 3.0 Hz, C₁₅), 131.3 (d, ¹J_{PC} = 97.5 Hz, C₁₂), 129.1 (d, ³J_{PC} = 12.0 Hz, C₁₄), 128.8 (s, C₄), 127.8 (s, C₇), 122.0 (s, C₉), 121.48 (s, C₅), 116.0 (s, C₆), 50.6 (d, ²J_{PC} = 3.5 Hz, C₁). IR (neat, cm⁻¹): 3230 (NH), 1676 (CO), 1518 (NH), 1435, 1234, 1218 (P=N), 1109. HRMS (ESI⁺): 462.1733 ([MH]⁺; C₂₉H₂₄N₃OP⁺; calcd 462.1730).

L^{Cy}H: 2-azido-N-(quinolin-8-yl)acetamide (2.18 g, 9.59 mmol) was dissolved in Et₂O (80 mL) and tricyclohexylphosphine (2.69 g, 9.59 mmol) was added portionwise under vigorous stirring resulting in a nitrogen evolution. The reaction mixture was stirred under nitrogen flux during 1 h. A white precipitate appeared rapidly after the addition. The white solid was filtered, washed with petroleum ether (3 x 40 mL), and then dried *in vacuo* to yield **L^{Cy}H** as a white solid (3.50 g, 76 %). ³¹P{¹H} NMR (CD₂Cl₂): δ 28.2 (s). ¹H NMR (CD₂Cl₂): δ 12.22 (bs, 1H, NH), 8.86 – 8.76 (m, 2H, H_{6,10}), 8.14 (dd, ³J_{HH} = 8.5 Hz, ⁴J_{HH} = 1.5 Hz, 1H, H₈), 7.59 – 7.37 (m, 3H, H_{4,5,7}), 3.97 (d, ³J_{PH} = 11.5 Hz, 2H, H₁), 2.31 – 1.21 (m, 33H, H₁₂₋₁₅). ¹³C{³¹P} NMR (CD₂Cl₂): δ 175.3 (s, C₂), 148.6 (s, C₁₀), 139.8 (s, C₁₁), 136.4 (s, C₈), 136.0 (s, C₃), 128.7 (s, C₄), 127.7 (s, C₇), 121.9 (s, C₉), 121.3 (s, C₅), 116.1 (s, C₆), 51.9 (s, C₁), 35.4 (s, C_{Cy}), 27.9 (s, C_{Cy}), 27.8 (s, C_{Cy}), 26.9 (s, C_{Cy}). IR (cm⁻¹): 3223 (NH), 2924 (CH), 2843 (CH), 2784 (CH), 1674 (CO), 1514 (NH), 1443 (CC_{Ar}), 1249, 1203 (P=N), 1172. Anal. Calcd for C₂₉H₂₄N₃OP: C, 72.62; H, 8.83; N, 8.76. Found: C, 72.78; H, 8.95; N, 8.87.

2: **L^{Pb}H** (0.185 g, 0.4 mmol) was dissolved in dichloromethane (10 mL) and KHMDS (0.199 g, 0.4 mmol) was then added. The dark brownish reaction mixture was stirred during 30 min and PdCl₂ (0.071 g, 0.4 mmol) was added. After overnight stirring at 40 °C, the reaction mixture was filtered. The volume was reduced to *ca.* 5 mL and 10 mL of Et₂O was layered above to yield crystals of **2** which were dried under vacuum (0.12 g, 50 %). ³¹P{¹H} NMR (CD₂Cl₂): δ 33.7 (s). ¹H-NMR (CD₂Cl₂): δ 8.82 (dd, ³J_{HH} = 5.0 Hz, ⁴J_{HH} = 1.5 Hz, 1H, H₁₀), 8.26 (dd, ³J_{PH} = 8.5 and 1.5 Hz, 1H, H₈), 7.99 – 7.89 (m, 6H, H₁₃), 7.75 – 7.52 (m, 11H, H_{Ar}), 7.40 – 7.31 (m, 2H, H_{Ar}), 3.73 (d, ³J_{PH} = 4.5 Hz, 2H, H₁). ¹³C NMR (CD₂Cl₂): δ = 179.8 (d, ³J_{PC} = 20.0 Hz, C₂), 149.5 (s, C₁₀), 147.8 (s, C₁₁), 146.8 (s), 138.8 (s), 134.4 (d, ²J_{PC} = 9.5 Hz, C₁₃), 133.3 (d, ⁴J_{PC} = 3.0 Hz, C₁₅), 130.6 (s), 129.6 (s), 129.1 (d, ³J_{PC} = 12.5 Hz, C₁₄), 127.3 (d, ¹J_{PC} = 102.0 Hz, C₁₂), 121.7 (s), 120.2 (s), 120.0 (s), 60.9 (s, C₁). IR (neat, cm⁻¹): 3051 (CH), 1618 (CO), 1501 (CC_{Ar}), 1433 (CC_{Ar}), 1390, 1108, 1106. HRMS (ESI⁺): 462.1737 ([L^{Pb}H]⁺; C₂₉H₂₄N₃OP⁺; calcd 462.1730), 566.0606 ([M-Cl]⁺; C₂₉H₂₃N₃OPP⁺; calcd 566.0619). Anal. Calcd for C₂₉H₂₃Cl₂N₃OPP⁺: C, 57.82; H, 3.85; N, 6.98. Found: C, 57.60; H, 4.02; N, 6.82.

3: A schlenk flask was charged with **L^{Pb}H** (0.230 g, 0.5 mmol), THF (10 mL), triethylamine (77 μL, 0.55 mmol) and [NiCl₂(DME)] (0.110 g, 0.5 mmol). The reaction mixture was stirred overnight at 50 °C. Then, volatiles were evaporated and dichloromethane (10 mL) was

added. This solution was washed with water (3x10 mL) and then evaporated. The obtained orange to red solid was then washed with pentane (2x10 mL) and dried *in vacuo* to yield **3** (0.248 g, 90 %). ³¹P{¹H} NMR (CD₂Cl₂): δ 35.9 (s). ¹H-NMR (CD₂Cl₂): δ 8.52 (d, ³J_{HH} = 7.5 Hz, 1H, H₆), 8.30 (d, ³J_{HH} = 5.0 Hz, 1H, H₁₀), 8.14 (d, ³J_{HH} = 8.5 Hz, 1H, H₈), 8.04 (dd, ³J_{PH} = 12.5, ³J_{HH} = 7.5 Hz, 6H, H₁₃), 7.74 – 7.49 (m, 9H, H_{14,15}), 7.42 (t, ³J_{HH} = 7.5 Hz, 1H, H₅), 7.30 – 7.13 (m, 2H, H_{4,9}), 3.18 (d, ³J_{PH} = 4.5 Hz, 2H, H₁). ¹³C NMR (CD₂Cl₂): δ = 180.0 (d, ³J_{PC} = 20.5 Hz, C₂), 150.5 (s, C₁₀), 146.7 (s, C₇), 145.2 (s, C₁₁), 138.4 (s, C₈), 134.2 (d, ²J_{PC} = 9.5 Hz, C₁₃), 132.9 (d, ⁴J_{PC} = 3.0 Hz, C₁₅), 129.5 (s, C₅), 129.3 (s, C₃), 129.0 (d, ³J_{PC} = 12.5 Hz, C₁₄), 128.5 (d, ¹J_{PC} = 102.0 Hz, C₁₂), 121.5 (s, C₄), 118.7 (s, C₉), 118.6 (s, C₆), 58.7 (s, C₁). IR (neat, cm⁻¹): 3044 (CH), 1617 (CO), 1503, 1437 (CC_{Ar}), 1403 (CC_{Ar}), 1258 (P=N), 1125, 1105. HRMS (ESI⁺): 462.1732 ([L^{Pb}H]⁺; C₂₉H₂₄N₃OP⁺; calcd 462.1730), 518.0918 ([M-Cl]⁺; C₂₉H₂₃N₃OPN⁺; calcd 518.0927).

5: **L^{Pb}H** (0.346 g, 0.75 mmol) was dissolved in toluene (15 mL) and [Ni(COD)₂] (0.215 g, 0.78 mmol) was added. After overnight stirring at 60 °C, the dark orange reaction mixture is filtered. Toluene was evaporated under vacuum. The obtained reddish solid is then washed with Et₂O (2 x 15 mL) and volatiles were removed *in vacuo* to yield **5** as a red solid (0.198 g, 51 %). ³¹P{¹H} NMR (THF-d₈): δ 72.4 (s). ¹H NMR (THF-d₈): δ 9.10 (dd, ³J_{HH} = 8.0 Hz, ⁴J_{HH} = 1.5 Hz, 1H, H₁₀), 8.27 (dd, ³J_{HH} = 8.0 Hz, ⁴J_{HH} = 1.5 Hz, 1H, H₈), 7.65 – 7.51 (m, 4H, m-CH_{Ph2}), 7.47 (t, ³J_{HH} = 8.0 Hz, 1H, H₅), 7.44 – 7.36 (m, 2H, p-CH_{Ph2}), 7.35 – 7.24 (m, 5H, H₉ and m-CH_{Ph2}), 7.24 – 7.06 (m, 4H, H_{4,6} and m-CH_{Ph}), 6.81 – 6.62 (m, 3H, CH_{Ph}), 3.82 (vp, ²J_{PH} = 8.0 Hz, ³J_{HH} = 5.0 Hz, 1H, NH), 3.68 (dd, ³J_{PH} = 24.0 Hz, ³J_{HH} = 5.0 Hz, 2H, H₁). ¹³C NMR (THF-d₈): δ 175.1 (s, C₂), 158.1 (d, ²J_{PC} = 54.5 Hz, C^{IV}_{Ph}), 151.2 (d, ³J_{PC} = 2.5 Hz, C₁₁), 149.7 (s, C₆), 145.6 (s, C₃), 139.9 (d, ⁴J_{PC} = 2.0 Hz, m-CH_{Ph}), 139.3 (s, C₈), 134.5 (d, ¹J_{PC} = 57.0 Hz, C₁₂), 133.9 (d, ³J_{PC} = 10.5 Hz, C₁₄), 131.2 (d, ⁴J_{PC} = 2.0 Hz, p-CH_{Ph2}), 129.7 (s, C₅), 129.1 (s, C₇), 128.8 (d, ²J_{PC} = 10.0 Hz, C₁₃), 127.2 (d, ³J_{PC} = 3.0 Hz, o-CH_{Ph}), 123.5 (s, p-CH_{Ph}), 123.4 (d, ³J_{PC} = 1.0 Hz, C₁₀), 121.5 (d, ⁴J_{PC} = 2.0 Hz, C₄), 118.0 (s, C₉), 51.7 (d, ²J_{PC} = 3.0 Hz, C₁). IR (neat, cm⁻¹): 3209 (NH), 1577 (CO), 1555 (NH), 1460 (CC_{Ar}), 1378, 1341, 1095. Anal. Calcd for C₂₉H₂₄N₃NiOP: C, 66.96; H, 4.65; N, 8.08. Found: C, 67.15; H, 4.75; N, 8.14.

6: **5** (0.02 g, 0.039 mmol) was dissolved in THF-d₈ (0.5 mL) and transferred in a NMR tube adapted with a J. Young valve. CO gas (0.3 bar) was then added to the degassed frozen solution. NMR analyses were performed on this tube. Crystals of the compound were obtained from a liquid diffusion of cold Et₂O into the solution. After drying the powder was used without any further purification (0.02 g, 86 %). ³¹P{¹H} NMR (THF-d₈): δ = 70.0 (s). ¹H NMR (THF-d₈): δ 9.08 (d, ³J_{HH} = 8.0 Hz, 1H, H₁₀), 8.44 – 8.28 (m, 3H, H_{Ar}), 8.16 – 8.06 (m, 2H, H₁₄), 8.06 – 8.00 (m, 1H, H_{Ar}), 7.54 – 7.40 (m, 4H, H_{Ar}), 7.37 – 7.26 (m, 2H, H_{4,9}), 7.25 – 7.11 (m, 3H, H_{Ar}), 7.11 – 7.01 (m, 2H, H₁₃), 7.02 – 6.89 (m, 3H, H_{Ar}), 4.14 (bs, 1H, H₁), 3.97 (bt, ²J_{PH} = 17.0 Hz, 1H, N-H), 3.55 (observed by HSQC, H_{1b}). ¹³C NMR (THF-d₈): δ 256.6 (d, ²J_{PC} = 37.5 Hz, C_{OPh}), 185.3 (s, free CO), 174.8 (s, C₂), 150.4 (d, ³J_{PC} = 2.5 Hz, C₃), 149.3 (s, C₆), 145.2 (s, C₁₁), 140.8 (d, ³J_{PC} = 3.0 Hz, C^{IV}_{Ph}), 139.8 (s, C₈), 135.7 (d, ¹J_{PC} = 60.5 Hz, C₁₂), 134.9 (d, ³J_{PC} = 10.5 Hz, C₁₄), 132.3 (d, ⁴J_{PC} = 10.5 Hz, C₁₃), 131.4 (s, C₅), 130.1 (d, ⁴J_{PC} = 1.0 Hz, C₁₅), 130.0 (s, m-CH_{Ph}), 129.8 (s, C₇), 129.0 (s, o-CH_{Ph}), 128.5 (s, p-CH_{Ph}), 123.5 (s, C₁₀), 122.1 (d, ⁴J_{CP} = 2.0 Hz, C₄), 118.2 (s, C₉), 52.2 (d, ²J_{PC} = 3.0 Hz, C₁). IR (neat, cm⁻¹): 3293 (NH), 1600 (CO), 1587 (CO), 1563 (NH), 1465, 1095.

Computational details: Following a recent DFT study on a Ni-catalyzed reaction,²⁸ geometries (minima and transition states) were optimized at the M06 level²⁹ of theory at 333.15 K and 1 atm using the Gaussian 09 software package.³⁰ The double- ζ basis set (LANL2DZ ECP) was used for Ni.³¹ All other atoms were described by the 6-31G(d,p) basis set.³² Frequency calculations were conducted at this level. Single point energy calculations were carried out at the M06 level of theory using the triple- ζ def2-TZVPP basis set for all atoms.³³ Solvent correction for toluene was obtained with the CPCM model as implemented in Gaussian.³⁴ The values presented are solvent-corrected M06/TZVPP Gibbs free energies (ΔG_{333} , kcal/mol). The discussed charges are Mulliken ones.

X-ray crystallography: Data were collected at 150 K on a Bruker Kappa APEX II diffractometer using a Mo- κ ($\lambda=0.71069\text{\AA}$) X-ray source and a graphite monochromator. The crystal structures were solved using Shelxt³⁵ or oleix³⁶ and refined using Shelxl-97 or Shelxl-2014.³⁷ ORTEP drawings were made using ORTEP III³⁸ for Windows or Mercury. Details of crystal data and structure refinements are summarized in Table S1 and S2.

ASSOCIATED CONTENT

Supporting Information

Detailed X-ray data, NMR spectra, complete Gaussian reference, computed Cartesian coordinates, energies, and frequencies.

AUTHOR INFORMATION

Corresponding Author

Email: vincent.gandon@polytechnique.edu
audrey.auffrant@polytechnique.edu

Notes

The authors declare no competing financial interests.

ACKNOWLEDGMENT

The authors thank Ecole polytechnique and CNRS for financial support. The GDR Phosphore is acknowledged for the organization of regular fruitful meetings.

REFERENCES

- (a) *The chemistry of pincer ligands*. Morales-Morales, D.; Jensen, C. Eds.; Elsevier: 2007; (b) *Organometallic Pincer Chemistry in Topics in Organometallic Chemistry*. van Koten, G.; Milstein, D. Eds.; Springer-Verlag: Berlin Heidelberg, 2013; Vol. 40.
- (a) Flamigni, L.; Collin, J. P. Sauvage, J. P. Iridium terpyridine complexes as functional assembling units in arrays for the conversion of light energy. *Acc. Chem. Res.* **2008**, *41*, 857-871; (b) Sakamoto, R.; Katagiri, S.; Maeda, H. Nishihara, H. Bis(terpyridine) metal complex wires: Excellent long-range electron transfer ability and controllable intrawire redox conduction on silicon electrode. *Coord. Chem. Rev.* **2013**, *257*, 1493-1506; (c) Wei, C. Y.; He, Y.; Shi, X. D. Song, Z. G. Terpyridine-metal complexes: Applications in catalysis and supramolecular chemistry. *Coord. Chem. Rev.* **2019**, *385*, 1-19.
- (a) Chirik, P. J. Iron- and Cobalt-Catalyzed Alkene Hydrogenation: Catalysis with Both Redox-Active and Strong Field Ligands. *Acc. Chem. Res.* **2015**, *48*, 1687-1695; (b) Small, B. L. Discovery and Development of Pyridine-bis(imine) and Related Catalysts for Olefin Polymerization and Oligomerization. *Acc. Chem. Res.* **2015**, *48*, 2599-2611.
- (a) Gade, L. H. Mountford, P. New transition metal imido chemistry with diamido-donor ligands. *Coord. Chem. Rev.* **2001**, *216*, 65-97; (b) Belda, O. Moberg, C. Bispyridylamides - coordination chemistry and applications in catalytic reactions. *Coord. Chem. Rev.* **2005**, *249*, 727-740; (c) Halcrow, M. A. The synthesis and coordination chemistry of 2,6-bis(pyrazolyl)pyridines and related ligands - Versatile terpyridine analogues. *Coord. Chem. Rev.* **2005**, *249*, 2880-2908; (d) Gunanathan, C. Milstein, D. Metal-Ligand Cooperation by Aromatization-De aromatization: A New Paradigm in Bond Activation and "Green" Catalysis. *Acc. Chem. Res.* **2011**, *44*, 588-602; (e) McPherson, J. N.; Das, B. Colbran, S. B. Tridentate pyridine-pyrrolide chelate ligands: An under-appreciated ligand set with an immensely promising coordination chemistry. *Coord. Chem. Rev.* **2018**, *375*, 285-332; (f) Wang, Z.; Solan, G. A.; Zhang, W. J. Sun, W. H. Carbocyclic-fused N,N,N-pincer ligands as ring-strain adjustable supports for iron and cobalt catalysts in ethylene oligo-/polymerization. *Coord. Chem. Rev.* **2018**, *363*, 92-108; (g) Alig, L.; Fritz, M. Schneider, S. First-Row Transition Metal

(De)Hydrogenation Catalysis Based On Functional Pincer Ligands. *Chem. Rev.* **2019**, *119*, 2681-2751.

5. Al-Benna, S.; Sarsfield, M. J.; Thornton-Pett, M.; Ormsby, D. L.; Maddox, P. J.; Brès, P. Bochmann, M. Sterically hindered iminophosphorane complexes of vanadium, iron, cobalt and nickel: a synthetic, structural and catalytic study. *J. Chem. Soc., Dalton Trans.* **2000**, 4247-4257.

6. (a) Cheisson, T.; Auffrant, A. Nocton, G. eta(5)-eta(1) Switch in Divalent Phosphaytterbocene Complexes with Neutral Iminophosphoranyl Pincer Ligands: Solid-State Structures and Solution NMR ^J_{Vb-P} Coupling Constants. *Organometallics* **2015**, *34*, 5470-5478; (b) Cheisson, T.; Ricard, L.; Heinemann, F. W.; Meyer, K.; Auffrant, A. Nocton, G. Synthesis and Reactivity of Low-Valent f-Element Iodide Complexes with Neutral Iminophosphorane Ligands. *Inorg. Chem.* **2018**, *57*, 9230-9240.

7. Cheisson, T. Auffrant, A. Versatile coordination chemistry of a bis(methyliminophosphoranyl)pyridine ligand on copper centres. *Dalton Trans.* **2014**, *43*, 13399-13409.

8. (a) Johnson, K. R. D.; Hannon, M. A.; Ritch, J. S. Hayes, P. G. Thermally stable rare earth dialkyl complexes supported by a novel bis(phosphinimine)pyrrole ligand. *Dalton Trans.* **2012**, *41*, 7873-7875; (b) Zamora, M. T.; Johnson, K. R. D.; Hänninen, M. M. Hayes, P. G. Differences in the cyclometalation reactivity of bisphosphinimine-supported organo-rare earth complexes. *Dalton Trans.* **2014**, *43*, 10739-10750.

9. MacNeil, C. S.; Glynn, K. E. Hayes, P. G. Facile Activation and Deoxygenative Metathesis of CO. *Organometallics* **2018**, *37*, 3248-3252.

10. (a) Rong, W.; Cheng, J.; Mou, Z.; Xie, H. Cui, D. Facile Preparation of a Scandium Terminal Imido Complex Supported by a Phosphazene Ligand. *Organometallics* **2013**, *32*, 5523-5529; (b) Rong, W.; He, D.; Wang, M.; Mou, Z.; Cheng, J.; Yao, C.; Li, S.; Trifonov, A. A.; Lyubov, D. M. Cui, D. Neutral binuclear rare-earth metal complexes with four μ^2 -bridging hydrides. *Chem. Commun.* **2015**, *51*, 5063-5065; (c) Rong, W.; Wang, M.; Li, S.; Cheng, J.; Liu, D. Cui, D. Insights into the Formation Process of Yttrium-Aluminum Bimetallic Alkyl Complexes Supported by a Bulky Phosphazene Ligand. *Organometallics* **2018**, *37*, 971-978.

11. Sarsfield, M. J.; Steele, H.; Helliwell, M. Teat, S. J. Uranyl bis-iminophosphorane complexes with in- and out-of-plane equatorial coordination. *Dalton Trans.* **2003**, 3443-3449.

12. (a) Johnson, K. R. D. Hayes, P. G. Synthesis and reactivity of dialkyl lutetium complexes supported by a novel bis(phosphinimine)carbazole pincer ligand. *Organometallics* **2009**, *28*, 6352-6361; (b) Johnson, K. R. D. Hayes, P. G. Kinetic and Mechanistic Investigation of Metallacycle Ring Opening in an Ortho-Metalated Lutetium Aryl Complex. *Organometallics* **2011**, *30*, 58-67.

13. Hänninen, M. M.; Zamora, M. T.; MacNeil, C. S.; Knott, J. P. Hayes, P. G. Elucidation of the resting state of a rhodium NNN-pincer hydrogenation catalyst that features a remarkably upfield hydride 1H NMR chemical shift. *Chem. Commun.* **2016**, *52*, 586-589.

14. (a) Cariou, R.; Graham, T. W. Stephan, D. W. Synthesis and reactivity of nickel-hydride amino-bis-phosphinimine complexes. *Dalton Trans.* **2013**, *42*, 4237-4239; (b) Cariou, R.; Graham, T. W.; Dahcheg, F.; Stephan, D. W. Oxidative addition of aryl halides: routes to mono and dimetallic nickel amino-bis-phosphinimine complexes. *Dalton Trans.* **2011**, *40*, 5419-5422; (c) Cariou, R.; Dahcheg, F.; Graham, T. W. Stephan, D. W. Mononuclear and dinuclear palladium and nickel complexes of phosphinimine-based tridentate ligands. *Dalton Trans.* **2011**, *40*, 4918-4925.

15. Alajarín, M.; López-Leonardo, C.; Llamas-Lorente, P.; Bautista, D. Jones, P. G. Synthesis and molecular structure of a new class of bi- and ter-dentate palladium complexes with iminophosphorane containing ligands. *Dalton Trans.* **2003**, 426-434.

16. (a) Marín, I. M. Auffrant, A. Phosphasalen vs. Salen Ligands: What Does the Phosphorus Change? *Eur. J. Inorg. Chem.* **2018**, *2018*, 1634-1644; (b) Cheisson, T. Auffrant, A. Palladium(II) complexes

- featuring a mixed phosphine-pyridine-iminophosphorane pincer ligand: synthesis and reactivity. *Dalton Trans.* **2016**, *45*, 2069-2078;
- (c) Dyer, H.; Picot, A.; Vendier, L.; Auffrant, A.; Le Floch, P. Sabo-Etienne, S. Tridentate and Tetradentate Iminophosphorane-Based Ruthenium Complexes in Catalytic Transfer Hydrogenation of Ketones. *Organometallics* **2011**, *30*, 1478-1486; (d) Cao, T. P. A.; Labouille, S.; Auffrant, A.; Jean, Y.; Le Goff, X. F. Le Floch, P. Pd(II) and Ni(II) complexes featuring a "phosphasalen" ligand: synthesis and DFT study. *Dalton Trans.* **2011**, *40*, 10029-10037; (e) Cao, T. P. A.; Payet, E.; Auffrant, A.; Le Goff, X. F. Le Floch, P. Facile Synthesis of Bifunctional Ligands using LiCH₂PPh₂=NPh Obtained from PhNH-PPh₃⁺ Br⁻. *Organometallics* **2010**, *29*, 3991-3996.
17. Eberhardt, N. A. Guan, H. Nickel Hydride Complexes. *Chem. Rev.* **2016**, *116*, 8373-8426.
18. (a) Boro, B. J.; Duesler, E. N.; Goldberg, K. I. Kemp, R. A. Synthesis, Characterization, and Reactivity of Nickel Hydride Complexes Containing 2,6-C₆H₃(CH₂PR₂)₂ (R = tBu, cHex, and iPr) Pincer Ligands. *Inorg. Chem.* **2009**, *48*, 5081-5087; (b) Lansing, R. B.; Goldberg, K. I. Kemp, R. A. Unsymmetrical RPNPR' pincer ligands and their group 10 complexes. *Dalton Trans.* **2011**, *40*, 8950-8958; (c) Venkanna, G. T.; Tammineni, S.; Arman, H. D. Tonzetich, Z. J. Synthesis, Characterization, and Catalytic Activity of Nickel(II) Alkyl Complexes Supported by Pyrrole-Diphosphine Ligands. *Organometallics* **2013**, *32*, 4656-4663; (d) Kreye, M.; Freytag, M.; Jones, P. G.; Williard, P. G.; Bernskoetter, W. H. Walter, M. D. Homolytic H₂ cleavage by a mercury-bridged Ni(i) pincer complex [(PNP)Ni]₂{μ-Hg}. *Chem. Commun.* **2015**, *51*, 2946-2949; (e) Li, H. F.; Goncalves, T. P.; Zhao, Q. Y.; Gong, D. R.; Lai, Z. P.; Wang, Z. X.; Zheng, J. R. Huang, K. W. Diverse catalytic reactivity of a dearomatized PN³P*-nickel hydride pincer complex towards CO₂ reduction. *Chem. Commun.* **2018**, *54*, 11395-11398; (f) Oren, D.; Diskin-Posner, Y.; Avram, L.; Feller, M. Milstein, D. Metal-Ligand Cooperation as Key in Formation of Dearomatized Ni^{II}-H Pincer Complexes and in Their Reactivity toward CO and CO₂. *Organometallics* **2018**, *37*, 2217-2221.
19. Zhu, J.-F.; Yuan, H.; Chan, W.-H. Lee, A. W. M. A colorimetric and fluorescent turn-on chemosensor operative in aqueous media for Zn²⁺ based on a multifunctionalized spirobenzopyran derivative. *Org. Biomol. Chem.* **2010**, *8*, 3957-3964.
20. Alvarez, S. G. Alvarez, M. T. A Practical Procedure for the Synthesis of Alkyl Azides at Ambient Temperature in Dimethyl Sulfoxide in High Purity and Yield. *Synthesis* **1997**, *1997*, 413-414.
21. (a) Mitsuyo, F.; Kenji, I. Yoshio, I. Iminophosphorane Complexes of Palladium(II). *Bull. Chem. Soc. Jpn.* **1975**, *48*, 2044-2046; (b) Saplinova, T.; Lehnert, C.; Böhme, U.; Wagler, J. Kroke, E. Melem-and melamine-derived iminophosphoranes. *New J. Chem.* **2010**, *34*, 1893-1908.
22. Sgro, M. J. Stephan, D. W. Ni(II), Pd(II), and Pt(II) complexes of PNP and PSP tridentate amino-phosphine ligands. *Dalton Trans.* **2012**, *41*, 6791-6802.
23. Vreeken, V.; Siegler, M. A.; de Bruin, B.; Reek, J. N. H.; Lutz, M. van der Vlugt, J. I. C-H Activation of Benzene by a Photoactivated Ni(II)(azide): Formation of a Transient Nickel Nitrido Complex. *Angew. Chem. Int. Ed.* **2015**, *54*, 7055-7059.
24. Sgro, M. J. Stephan, D. W. Non-innocent reactivity of bis-phosphinimine pincer ligands in palladium complexes. *Dalton Trans.* **2011**, *40*, 2419-2421.
25. (a) Pu, X.; Hu, J.; Zhao, Y. Shi, Z. Nickel-Catalyzed Decarbonylative Borylation and Silylation of Esters. *ACS Catal.* **2016**, *6*, 6692-6698; (b) Zhao, H.-Y.; Gao, X.; Zhang, S. Zhang, X. Nickel-Catalyzed Carbonylation of Difluoroalkyl Bromides with Arylboronic Acids. *Org. Lett.* **2019**, *21*, 1031-1036.
26. (a) Ackerman, L. K. G.; Alvarado, J. I. M. Doyle, A. G. Direct C-C Bond Formation from Alkanes Using Ni-Photoredox Catalysis. *J. Am. Chem. Soc.* **2018**, *140*, 14059-14063; (b) Gutierrez, E.; Hudson, S. A.; Monge, A.; Nicasio, M. C.; Paneque, M. Ruiz, C. Organometallic derivatives of Ni(II) with poly(pyrazolyl)borate ligands. *J. Organomet. Chem.* **1998**, *551*, 215-227; (c) Carmona, E.; Paneque, M. Poveda, M. L. Synthesis and characterization of some new organometallic complexes of nickel(II) containing trimethylphosphine. *Polyhedron* **1989**, *8*, 285-291.
27. The Ni benzoyl complexes described in the CCDC correspond to numbers 1837039, 901728, 901728, 901728, 901728, and 901728.
28. Jain, P.; Pal, S. Avasare, V. Ni(COD)₂-Catalyzed ipso-Silylation of 2-Methoxynaphthalene: A Density Functional Theory Study. *Organometallics* **2018**, *37*, 1141-1149.
29. Zhao, Y. Truhlar, D. G. A new local density functional for main-group thermochemistry, transition metal bonding, thermochemical kinetics, and noncovalent interactions. *J. Chem. Phys.* **2006**, *125*.
30. Frisch, M. J. et al. Gaussian 09, Revision D.01. Gaussian inc., Wallingford CT, 2013.
31. (a) Hay, P. J. Wadt, W. R. Ab initio effective core potentials for molecular calculations- potentials for the transition metal atoms Sc to Hg. *J. Chem. Phys.* **1985**, *82*, 270-283; (b) Hay, P. J. Wadt, W. R. Ab initio effective core potentials for molecular calculations- potentials for K to Au including the outermost core orbitals. *J. Chem. Phys.* **1985**, *82*, 299-310; (c) Wadt, W. R. Hay, P. J. Ab initio effective core potentials for molecular calculations- potentials for main group elements Na to Bi. *J. Chem. Phys.* **1985**, *82*, 284-298; (d) Dunning Jr, T. H. Hay, P. J. *Modern Theoretical Chemistry*. Schaefer III, H. F. Eds.; Plenum: New York, 1997.
32. (a) Krishnan, R.; Binkley, J. S.; Seeger, R. Pople, J. A. Self-consistent molecular-orbital methods. 20 basis set for correlated wave-functions. *J. Chem. Phys.* **1980**, *72*, 650-654; (b) McLean, A. D. Chandler, G. S. Contracted gaussian-basis sets for molecular calculations. 1. 2nd atoms, Z = 11-18. *J. Chem. Phys.* **1980**, *72*, 5639-5648.
33. (a) Weigend, F. Ahlrichs, R. Balanced basis sets of split valence, triple zeta valence and quadruple zeta valence quality for H to Rn: Design and assessment of accuracy. *Phys. Chem. Chem. Phys.* **2005**, *7*, 3297-3305; (b) Weigend, F. Accurate Coulomb-fitting basis sets for H to Rn. *Phys. Chem. Chem. Phys.* **2006**, *8*, 1057-1065.
34. Scalmani, G. Frisch, M. J. Continuous surface charge polarizable continuum models of solvation. I. General formalism. *J. Chem. Phys.* **2010**, *132*.
35. Sheldrick, G. SHELXT - Integrated space-group and crystal-structure determination. *Acta Cryst. Section A* **2015**, *71*, 3-8.
36. Dolomanov, O. V.; Bourhis, L. J.; Gildea, R. J.; Howard, J. A. K. Puschmann, H. OLEX2: a complete structure solution, refinement and analysis program. *J. Appl. Crystallogr.* **2009**, *42*, 339-341.
37. Sheldrick, G. Crystal structure refinement with SHELXL. *Acta Cryst. Section C* **2015**, *71*, 3-8.
38. Farrugia, L. J. *ORTEP-3 program*, Department of Chemistry, University of Glasgow: 2001.

